Open Archive Toulouse Archive Ouverte (OATAO)

OATAO is an open access repository that collects the work of Toulouse researchers and makes it freely available over the web where possible.

This is an author-deposited version published in: http://oatao.univ-toulouse.fr/
Eprints ID: 10862

Any correspondence concerning this service should be sent to the repository administrator: staff-oatao@inp-toulouse.fr

Analysis of the mesoscopic high cycle fatigue strength of FCC metals with polycrystalline plasticity and extreme value probability methods

A. Hor[1,a] , N. Saintier[1,b] , C. Robert[2,c] T. Palin-Luc[1,d] and F. Morel[2,e]

[1] Arts et Métiers ParisTech, I2M - CNRS, Esplanade des Arts et Métiers 33405 Talence, France

[2] Arts et Métiers ParisTech, LAMPA, 2 bd du Ronceray 49035 Angers, France

[a] anis.hor@ensam.eu, [b] nicolas.saintier@ensam.eu, [c] camille.robert@ensam.eu,

[d] thierry.palin-luc@ensam.eu, [e] franck.morel@ensam.eu

Abstract. This study analyzes the influence of microstructure properties on the extreme value distributions of the fatigue indicator parameter (FIP) corresponding to the multiaxial HCF Dang Van criterion. The following loading cases are considered: uniaxial loading, proportional and non-proportional multiaxial loadings. The mesoscopic FIP determined from FE calculations on 2D polycrystalline synthetic aggregates using the ZeBuLoN code. The approach adopted in this work is to replace the RVE by random microstructure elements that can be considered as "statistical volume element" (SVE) [1]. A set of extreme values is constructed by determining the maximum value of the FIP for each SVE. The type of extreme value distribution is analyzed with a generalized extreme value function and is shown to follow a Gumbel type distribution. The shape factors of this distribution are compared for the different loading conditions. This comparison shows the limitations of the used criterion, especially in the case of multiaxial loadings. The effect of anisotropy on these distributions is finally investigated by comparing the results of two types of texture (isotropic and rolling). The introduction of a preferential texture reduces the shape factor and the criterion applied with the classic stress field becomes conservative, and also decreases the scatter parameter of the extreme value distributions of the FIP.

Introduction
In one literature, methods for determining the fatigue behavior based on multiscale modeling estimate that the fatigue strength depends on the extreme value statistics of a single microstructure attribute [2] (for example inclusion size). This is only valid when the considered element of microstructure is a representative volume element (RVE). A RVE is the smallest volume element whose averaged behavior converges towards the macroscopic behavior material. Although the definition of the RVE is possible for some deterministic behavior aspects (such as elastoplastic behavior), it is difficult to evaluate an RVE for HCF behavior which is macroscopically highly dispersed. Therefore the use of extreme values of a single microstructure (lower than the RVE with regards to the fatigue behavior) does not take into account the contribution of the microstructural dispersion in the HCF response. To solve this issue, Liao [3] used the Monte Carlo method to create the statistical volume element (SVE) of a microstructure with a random distribution of grain sizes and orientations. Despite considering elastic behavior of crystal only, Liao showed a good correlation between the results obtained by modeling the extreme value probability with a Fréchet distribution and experimental results for 2024 aluminum alloy. Recently, McDowell et al. [1, 4] introduced a new framework taking into account the effects of neighborhood through the extreme values of the marked correlation functions [5] to quantify the influence of microstructure on the

fatigue limit and the contribution of interactions in the microstructure in the case of uniaxial loading. McDowell used the Gumbel distribution to describe the extreme value probability of the studied parameters.

The aim of this study is to analyze the influence of microstructure features (morphology and orientation) on the extreme value distributions of the Dang Van fatigue indicator parameter (FIP) under uniaxial and multiaxial loadings. The adopted approach is summarized in fig.1.
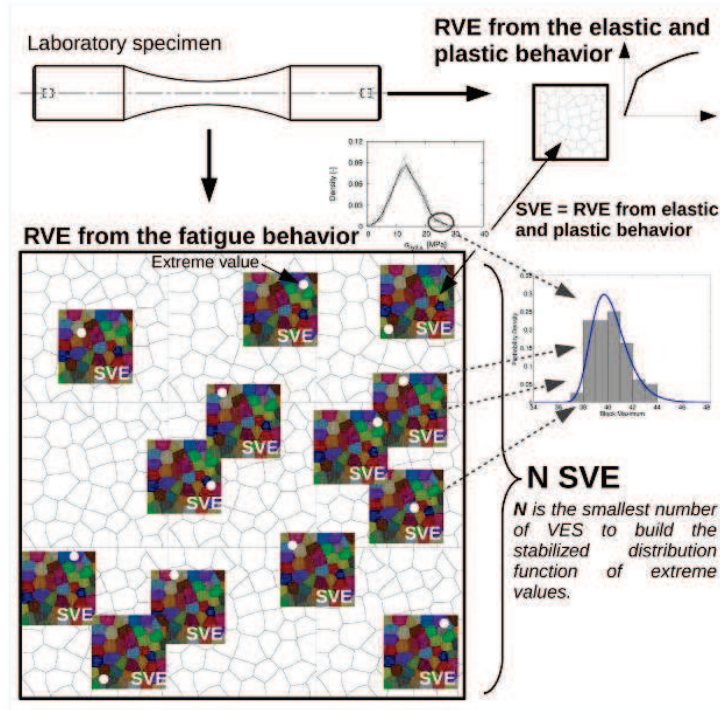

Fig.1. Schematic representation of the approach adopted in this study

Numerical model
Material behaviour. The model material considered in this work is pure copper. The face-centered cubic crystal structure reduces the computation time because of the reduced number of slip systems (12 <111> {110} slip systems on a fcc structure). The behavior is modeled by cubic elasticity and crystal plasticity constitutive law. The cubic elasticity constants are $C_{11} = 159\,GPa$, $C_{12} = 121.9\,GPa$ and $C_{44} = 80.9\,GPa$ (Voigt notation). The crystal plasticity model used in this work is the one introduced by Meric and Cailletaud [6]. The constitutive relations are defined in Table 1.

Table 1. Constitutive relations of the crystal plasticity behavior

Plastic flow	$\dot{\gamma}^s = \left(\dfrac{\left\| \tau^s - x^s \right\| - r^s}{K} \right) sign(\tau^s) = \dot{v}^s sign(\tau^s)$
Isotropic hardening	$r^s = r_0 + Q \sum\limits_{r} h^{rs} \left(1 - \exp\{-b\,v^s\} \right)$
Kinematic hardening	$x^s = c\alpha^s$ with $\dot{\alpha}^s = \dot{\gamma}^s - d\dot{v}^s \alpha^s$

γ^s and τ^s respectively represent the plastic slip and the resolved shear stress of the slip system s. These two variables are related to the stress and plastic strain tensors by the following relations:

$$\tau^s = \underline{\underline{m}}^s : \underline{\underline{\sigma}} \quad \text{and} \quad \underline{\underline{\dot{\varepsilon}}}^{pl} = \sum_s \dot{\gamma}^s \underline{\underline{m}}^s \tag{1}$$

where $\underline{\underline{m}}^s$ is the orientation tensor, computed on each slip system s by the tensorial product of the unit normal vector to the slip plane $\underline{n}^s$ and the unit vector characterized the slip direction $\underline{l}^s$:

$$\underline{\underline{m}}^s = \frac{1}{2}\left(\underline{n}^s \otimes \underline{l}^s + \underline{l}^s \otimes \underline{n}^s\right) \tag{2}$$

The material parameters $K\left[MPa.s^{1/n}\right]$, n, $r_0[MPa]$, $Q[MPa]$, b, $c[MPa]$ and d and the interaction matrix components have been identified on a high purity copper [7]. They are presented in Table 2.

Table 2. Material parameters of pure copper from [7]

K	n	r_0	Q	b	c	d	h_0	h_1	h_2	h_3	h_4	h_5
8	20	15	4	12	32000	900	1	1	0.2	90	3	2.5

Equiaxed morphology modeling. The simulations performed in this work used a 2D periodic microstructure following the procedure presented in [8]. To have a reasonable computation time, each computed SVE contain 200 equiaxed grains and 160 elements /grain in average. The microstructure and the mesh are periodic along the two axes. The polycrystalline aggregates here after were subjected to cyclic loading levels corresponding to the median experimental fatigue strength at 10^7 cycles of pure copper determined by Lukas et al. [9]. To determine the combined loading levels equivalent to the fatigue strength at 10^7 cycles, the Crossland criterion [10] was used. The fatigue limits used in this study are shown in Table 3. The loading ratio is $R_\Sigma = \Sigma_{min} / \Sigma_{max} = -1$, and in the case of the combined tension-torsion loading, the biaxiality ratio is $\Sigma_a / T_a = 1$. Computations were performed under imposed mean stress loading conditions and periodic displacement on the contour of the aggregate. The calculations were performed for 10 cycles using ZeBuLoN FE code. It was assumed that the macroscopic and mesoscopic behaviors are almost stabilized at the end of the tenth cycle.

Table 3. Macroscopic tension and shear stress amplitudes used for the different loading conditions

	Tension (TE)	Torsion (TO)	Tension-Torsion (TT0, TT45, TT90)
$\Sigma_a\,[MPa]$	56	0	30
$T_a\,[MPa]$	0	36	30

Crystallographic texture and anisotropy. In the present work, the grain shape is fixed (equiaxed) and were two types of texture investigated. First, an isotropic material was considered. The computed grain orientation sets were obtained by random samplings of 200 crystal orientations among the possible orientations in Euler space defined by three angles ($\varphi_1, \phi, \varphi_2$). Secondly, a textured material was considered. The random samplings were made from the marked orientations of an experimental rolling texture. These marked orientations correspond to different orientations of the γ fiber developed by deformation during the rolling process. Examples of the generated {100}, {110} and {111} pole figures for (a) isotropic and (b) anisotropic microstructure are given in Fig.2.
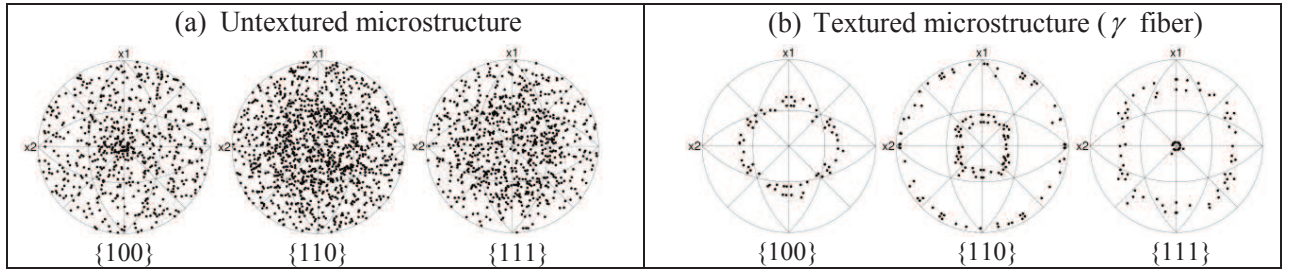
Fig.2. {100}, {110} and {111} stereographic pole figures of computed microstructures in the case of (a) untextured and (b) textured microstructure (x1 is a transverse direction and x2 is a rolling direction).

Dang Van Fatigue indicator parameter

The stress based critical plane Dang Van fatigue criterion [11] was chosen as it is largely used in the literature. It has given rise to several developments [12, 13] of meso-macro HCF criteria. It was developed in a homogeneous continuum medium mechanics framework considering an elastic shakedown hypothesis. The critical plane is determined from all the possible planes. In this study the Dang Van criterion is computed for each grain considering its local stress state (obtained by FE computation) and its orientation. The planes and the directions on which the criterion is evaluated correspond to the slip systems of the grain. The formulation introduces an equivalent stress (also known as fatigue indicator parameter FIP):

$$I_{DV} = \max_{s} \left\{ \max_{t} \left(\left\| \tau_r^s(t) \right\| + K_{DV}\sigma_{hyd}(t) \right) \right\} \le I_{DV}^{th} \quad (3)$$

where $\sigma_{hyd}(t)$ is the hydrostatic stress, $\left\| \tau_r^s(t) \right\|$ is the resolved shear stress recentered (using the circumscribed circle method) for the slip system s. The threshold value I_{DV}^{th} of I_{DV} and the material parameter K_{DV} are identified from the median experimental macroscopic fatigue limits at 10^7 cycles [9] using:

$$K_{DV} = 3\left(\frac{t_{-1}}{f_{-1}} - \frac{1}{2} \right); \quad I_{DV}^{th} = t_{-1} \quad (4)$$

where f_{-1} and t_{-1} are respectively the fatigue strength at 10^7 cycles in terms of fully reversed tensile and shear stress [9]. The material parameters determination from the macroscopic experimental results of the tests is disputable. The Fig.3 illustrates the mesoscopic loading path in the sense of Dang Van criterion (with $I_{DV}^{th} = 36.15\,MPa$ determined experimentally) for the five loading cases.

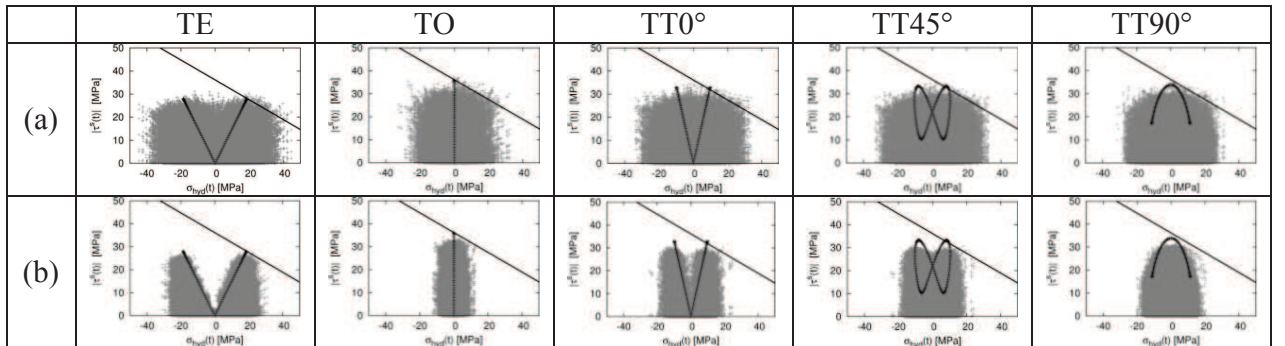Fig.3. Mesoscopic loading path in the Dang Van space $(\sigma_{hyd}(t), |\tau^s(t)|)$ at the tenth cycle (with FE and polycrystal plasticity in gray dots and acending to the classical continuum mechanics in black dots) for (a) untextured and (b) textured microstructure.

The assumption used in the Dang Van criterion for meso-macro scale changement (Lin-Taylor hypothesis with the same macro and meso isotropic elastic behavior) leads to the equality between mesoscopic and macroscopic hydrostatic stress [11]. But Fig.3 shows a large scatter of hydrostatic stress at the grain scale. The results obtained for the textured and untextured cases show considerable variation of hydrostatic stress from one grain to another. Furthermore, the authors have shown [14] that the main difference between the continuum approach and the crystal plasticity approach used in this work is in the elastic anisotropy of grains. Moreover, for the same imposed macroscopic stress, the introduction of a preferential orientation (texture) decreases the scatter of the load paths. The greatest mesoscopic equivalent Dang Van stress is slightly reduced too. Note that for all the investigated load cases the critical paths are symmetric with regard to an average shear stress because plasticity is low and the residual stresses are negligible.

In the following, the fatigue strengths at 10^7 cycles at the mesoscopic scale are computed by considering the critical grain. These mesoscopic quantities are very sensitive to the grain morphology and orientation in the polycrystalline aggregate. They are located in the tail distributions (see Fig.4). One way to study the distribution of these quantities and the microstructure effect on the variability of these quantities is to use the extreme value probability. As done by Przybyla et al. [1] the database constructed by a lot of numerical simulations on several SVE allows the authors to build the statistical distribution of the fatigue indicator parameter (FIP). The SVE gives the grain exhibiting the highest FIP (extreme value).
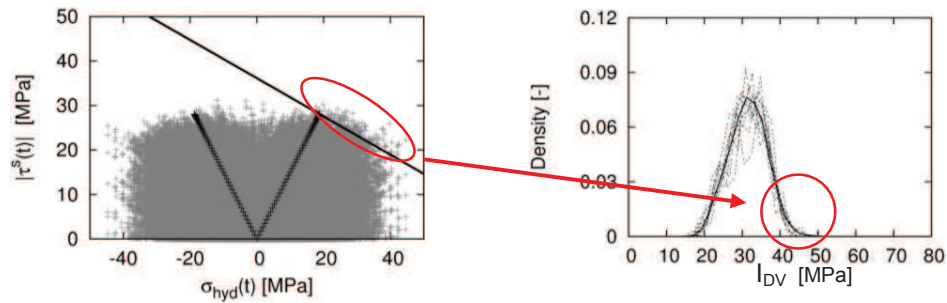

Fig.4. Localization of the extreme values in the tails of the Dang Van FIP distribution.

Probabilistic framework and extreme value probability
Let us consider a random variable x with the distribution function $F_X(x)$. The n extreme realizations in n samples of the random variable can be defined as:
$$Y_n = \max(X_1, X_2, ..., X_n) \tag{5}$$
The distribution function of Y_n is defined as:
$$F_{Y_n}(y) \equiv P(Y_n \leq y) = P(X_1 \leq y, X_2 \leq y, ..., X_n \leq y) \tag{6}$$
The extreme value theorem is similar to the Central Limit Theorem (CLT) reported in the sum of a series of random variables with same expected value and same variance that converges to a normal distribution.

According to the *Fisher-Tippet theorem*, if there exist two real normalizing sequences $(a_n)_{n \geq 1} > 0$ and $(b_n)_{n \geq 1}$ and a non-degenerate distribution (not reduced to a point) G such that :
$$P\left(\frac{Y_n - b_n}{a_n} \leq x\right) = F^n(a_n x + b_n) \xrightarrow[n \to +\infty]{} G(x) \tag{7}$$
G is necessarily one of three types of distributions: Fréchet, Weibull or Gumbel.

Jenkinson [15] combined the three limit distributions in a single parametric form called Generalized Extreme Value (GEV) distribution depending on a single parameter ξ:

$$G_\xi(x) = \begin{cases} \exp\left(-(1+\xi x)^{-\frac{1}{\xi}}\right) & si\ \xi \neq 0, \forall x / 1 + \xi x > 0 \\ \exp(-\exp(-x)) & si\ \xi = 0 \end{cases} \tag{8}$$

The ξ parameter is called extreme index. Its sign indicates the type of asymptotic distribution: Weibull ($\xi < 0$), Gumbel ($\xi = 0$) or Fréchet ($\xi > 0$). The variable $(Y_n - b_n)/a_n$ is called normalized maximum of the random variable x. $\mu \equiv b_n$ is considered as the average of the extreme value distribution whereas $s \equiv a_n$ is similar to the standard deviation as a measure of the dispersion of this distribution. These parameters are also called shape factors of the distribution.

The first step in the application of the extreme value probability consists in determining the type of attraction domain (AD) of the studied distribution: Gumbel, Fréchet or Weibull. Testing Quantile-Quantile plot graph (QQplot) can indicate qualitatively the type of attraction domain [14]. There are not many testing hypothesis to study the attraction domain of extreme value distributions, only one test was found in the literature: the ET test for the AD (Gumbel) [16]. To answer the question: "what is the extreme value distribution of the considered fatigue indicator parameter (FIP)", we used the GEV distribution. The extreme index ξ is computed with the two shape factors of the distribution (μ and s) with the maximum likelihood method.

Finally, the database of extreme values was constructed in this work by determining the maximum value of the Dang Van FIP for each SVE (see Fig.1). Initially 80 samplings of SVE were performed as the combination of 8 random morphologies (equiaxed grains) and 10 random crystallographic orientations. Then after determining the minimum number of samplings that is sufficient to obtain a stabilized extreme value distribution function, in the second part of the study, the influence of the texture was studied with 25 SVE only (obtained by the combination of 5 morphologies and 5 crystallographic orientations sampled randomly from an experimental rolling texture). Due to the introduction of this anisotropy, two cases are considered according to the tensile axis: (i) the case of textured microstructure with tensile direction along x1 axis and (ii) the case of textured microstructure with tensile direction along x2 axis.

Results and discussions
After identifying the various parameters of the GEV with the maximum likelihood method with a confidence interval of 99%, we noticed that for all the studied cases (untextured and textured microstructure with tension along x1 or x2 directions) and for the five loading cases, the average value of extreme index was very close to zero with intervals containing always zero (bounded by the minimum and maximum values). An example of the range of this parameter and the two shape factors is illustrated in Fig.5 with two probability density functions and associated cumulative probability. Consequently, the Gumbel distribution function is the most suitable to reproduce the extreme value distributions of the Dang Van FIP.

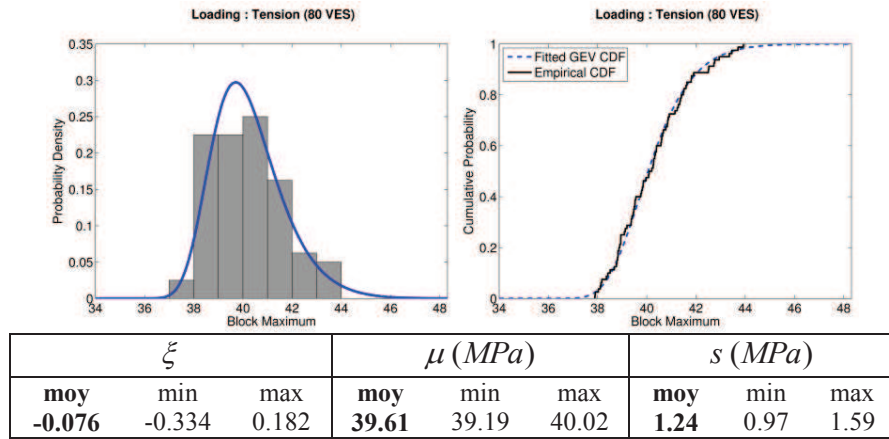| ξ			$\mu\,(MPa)$			$s\,(MPa)$		
moy	min	max	**moy**	min	max	**moy**	min	max
-0.076	-0.334	0.182	**39.61**	39.19	40.02	**1.24**	0.97	1.59

Fig.5. Probability density and cumulative probability determined with the maximum likelihood method (for the risk $\alpha = 0.01$) from the extreme values of the Dang Van FIP in tension ($R_\Sigma = -1$).

To evaluate the *sensitivity of the fatigue limit to the microstructure variability* and to determine the texture effect, three typical microstructures are studied: untextured, textured with tension in the transverse direction x1 and textured with tension in the rolling direction x2. In all cases, the shape factors of the Gumbel extreme value distributions of the Dang Van FIP, I_{DV}, were computed and analyzed.
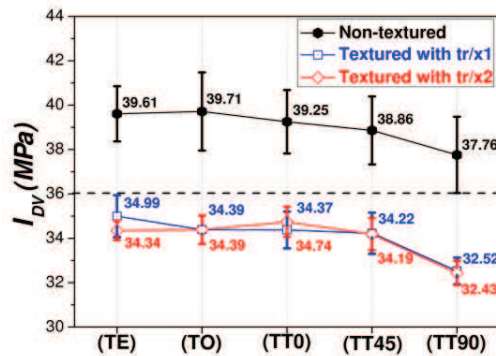

Fig.6. Shape factors $\mu\,(MPa)$ (symbols) and $s\,(MPa)$ (vertical bars) of the extreme value distributions of the Dang Van FIP, I_{DV}, for the five loading cases.

The introduction of a preferential texture reduces the parameter s (similar to the standard deviation) compared to the case of an isotropic texture for the five loading cases. This is explained by the mesoscopic stresses which are less heterogeneous due to the dominant orientations. Concerning the shape factor μ (similar to the average), for the five loading configurations this parameter exceeds the experimental macroscopic Dang Van criterion in the untextured microstructure case ($I_{DV}^{th} = 36.15\,MPa$ dotted line in Fig. 6). However, in the textured microstructure case, the macroscopic criterion is respected for simple and biaxial loadings. The symetry property of the orthotropic texture justifies that loading with a tensile direction in x1 or x2 give the same shape factors of the extreme value distribution.

In general, the introduction of a preferential texture has translated the shape factor of the Gumbel distribution to the bottom for the five load cases studied. This discrepancy may be due to the decrease in mesoscopic stresses coming from the deformation compatibility between neighboring grains resulting from the preferred orientations. However, this does not justify the decrease

compared to the macroscopic criterion excepted when the slip plane orientations given by the preferred orientations (corresponding to the γ fiber orientations) do not coincide for all the loading cases with plane orientations that maximizes the Dang Van FIP. Finally, in the experimental results of the literature, the macroscopic Dang Van criterion (based on continuum mechanics approach) is often more conservative in the case of simple loadings than under biaxial loadings. The adaptation of this criterion at the mesoscopic scale (crystal plasticity approach) shows that it is more conservative for combined tension-torsion loadings and even more conservative when the phase shift increases.

Conclusions and prospects

In this study, we constructed a database of extreme values of the Dang Van FIP. This database results from the FE simulations using several SVE (with 200 equiaxed grains randomly oriented and then respecting an experimental rolling texture). The application of this approach based on crystal plasticity coupled with probabilistic methods to study the distribution tails aims to analyze the sensitivity of the critical FIP to the microstructure features (morphology and texture) of pure copper. It has been shown that the extreme value distributions of the Dang Van FIP can be adequately represented by the Gumbel distribution. The identification of these distributions revealed that the experimental macroscopic fatigue parameters are not adequate at the mesoscopic scale. Indeed the shape factor μ (similar to the average) is always greater than the experimental median Dang Van threshold for the five loading configurations in the case of an equiaxed morphology and random texture. The introduction of a preferential texture reduces the shape factor and the criterion applied with the classic stress field (continuum mechanics) becomes conservative, and also decreases the dispersion parameter s. The use of a textured microstructure decreases the misorientation between grains. The stresses at the critical grain are reduced and the stress heterogeneity too. Consequently, the shape parameter of the extreme value distribution is decreased. This decreasing compared to the experimental macroscopic median threshold may be due to the incomplete representation of the Dang Van critical planes caused by the adaptation of this criterion at the mesoscopic scale.

References
[1]   C. P. Przybyla, R. Prasannavenkatesan, N. Salajegheh, and D. L. Mc-Dowell. Int. J. of Fatigue, 32(3): 512-525, 2010.
[2]   H.V. Atkinson and G. Shi. Prog. in Mater. Sci., 48: 457-520, 2003.
[3]   M. Liao. Eng. Frac. Mech., 76: 668-680, 2009.
[4]   C. P. Przybyla and D. L. McDowell. Int. J. of Plasticity, 26(3): 372-394, 2010.
[5]   Ryszard Pyrz. Mat. Sci. and Eng. : A, 177(1-2): 253-259, 1994.
[6]   L. Meric and G. Cailletaud. J. of Eng. Mater. and Tech., 113(1): 171-182, 1991.
[7]   C. Gérard, F. N'Guyen, N. Osipov, G. Cailletaud, M. Bornert, and D. Caldemaison. Comput. Mater. Sci., 46(3): 755-760, 2009.
[8]   C. Robert, N. Saintier, T. Palin-Luc, and F. Morel. Mécanique et Industries, 209-214, 2011.
[9]   P. Lukás and L. Kunz. Int. J. of Fatigue, 11(1): 55-58, 1989.
[10]   B. Crossland. Institution of Mechanical Engineers, pages 138-149, 1956. Proceedings of the International Conference on Fatigue of Metals, London.
[11]   K. Dang Van, B. Griveau, and O. Message. Mech. Eng. Publi. London, 479-496, 1989.
[12]   I.V. Papadopoulos. Int. J. of Fatigue, 16: 377-384, 1994.
[13]   F. Morel. Int. J. of Fatigue, 22: 101-119, 2000.
[14]   C. Robert, N. Saintier, T. Palin-Luc, and F. Morel, Mech. of Mater., 2012 (*submitted*).
[15]   A.F. Jenkinson. Quaterly Journal of the Royal Meteorological Society, 81, 1955.
[16]   M. Garrido. Phd of Joseph Fourier University, 2002.